Human Galectin-1 Improves Sarcolemma Stability and Muscle Vascularization in the mdx Mouse Model of Duchenne Muscular Dystrophy

Ryan D. Wuebbles,[1,2] Vivian Cruz,[2] Pam Van Ry,[1,2] Pamela Barraza-Flores,[1] Paul D. Brewer,[2] Peter Jones,[1] and Dean J. Burkin[1,2]

[1]Department of Pharmacology, Center for Molecular Medicine, University of Nevada, Reno School of Medicine, Reno, NV 89557, USA; [2]StrykaGen Corporation, Reno, NV 89557, USA

Duchenne muscular dystrophy (DMD) is a devastating disease caused by mutations in the dystrophin gene that result in the complete absence of dystrophin protein. We have shown previously that recombinant mouse Galectin-1 treatment improves physiological and histological outcome measures in the *mdx* mouse model of DMD. Because recombinant human Galectin-1 (rHsGal1) will be used to treat DMD patients, we performed a dose-ranging study and intraperitoneal or intravenous delivery to determine the efficacy of rHsGal1 to improve preclinical outcome measures in *mdx* mice. Our studies showed that the optimal dose of rHsGal1 delivered intraperitoneally was 20 mg/kg and that this treatment improved muscle strength, sarcolemma stability, and capillary density in skeletal muscle. We next examined the efficacy of intravenous delivery and found that a dose of 2.5 mg/kg rHsGal1 was well tolerated and improved outcome measures in the *mdx* mouse model. Our studies identified that intravenous doses of rHsGal1 exceeding 2.5 mg/kg resulted in toxicity, indicating that dosing using this delivery mechanism will need to be carefully monitored. Our results support the idea that rHsGal1 treatment can improve outcome measures in the *mdx* mouse model and support further development as a potential therapeutic agent for DMD.

INTRODUCTION

Duchenne muscular dystrophy (DMD) is a fatal X-linked genetic disease caused by mutations in the dystrophin gene. DMD affects approximately 1 in 5,000 males worldwide, with symptoms beginning early in childhood followed by progressive muscle loss. Patients are often confined to a wheelchair in their teenage years, with death occurring in their second or third decade of life from respiratory or cardiac failure.[1,2] The first-line treatment for DMD is corticosteroids, which transiently improve patient strength through a combination of inflammatory suppression and extracellular matrix alteration, but long-term treatment can have serious adverse effects.[3–8] New treatments are being developed for DMD and include exon-skipping oligonucleotides, gene editing, gene therapy, small molecules, and protein therapeutics.[9,10]

Recombinant Galectin-1 is a protein therapeutic agent recently shown to ameliorate disease progression in the *mdx* mouse model of DMD.[11] Endogenous Galectin-1 has diverse biological roles, many of which appear to be important for protecting distressed tissues.[12,13] Galectin-1 has been shown to be involved in the promotion of immune tolerance,[14] modulation of calcium channels,[15–17] enhancement of muscle regeneration,[18–22] enhancement of sarcolemma stabilization,[11,23] positive regulation of angiogenesis,[24,25] enhancement of neuromuscular junction stabilization,[26,27] and oxidative stress amelioration.[28] These protective activities are negative in the context of cancer, which has made Galectin-1 a target of cancer therapies.[29] However, together, these protective activities make Galectin-1 a strong candidate for the treatment of muscular dystrophies.

In this study, we produced highly purified recombinant human Galectin-1 (rHsGal1) and completed delivery and dose-ranging studies in the *mdx* mouse model of DMD. Our results demonstrate that weekly intraperitoneal dosing of 20 mg/kg rHsGal1 was optimal in *mdx* mice, which matched the previously published dosing and treatment schedule with recombinant mouse Galectin-1 (rMsGal1).[11] Beyond improvements in muscle strength and sarcolemma stability, we show increased muscle micro-vascularization suggesting another potential mechanism by which Galectin-1 treatment may improve dystrophic muscle function. Together, these results suggest that rHsGal1 is a potent biological agent that can improve preclinical outcome measures in a mouse model of DMD.

RESULTS

Human Galectin-1 Treatment Improves *mdx* Mouse Muscle Outcome Measures

We have previously shown positive effects in *mdx* mice of intraperitoneal (i.p.) injections with a His$_6$-tagged recombinant mouse

Correspondence: Dean J. Burkin, PhD, Department of Pharmacology, Center for Molecular Medicine, University of Nevada, Reno School of Medicine, Reno, NV 89557, USA.
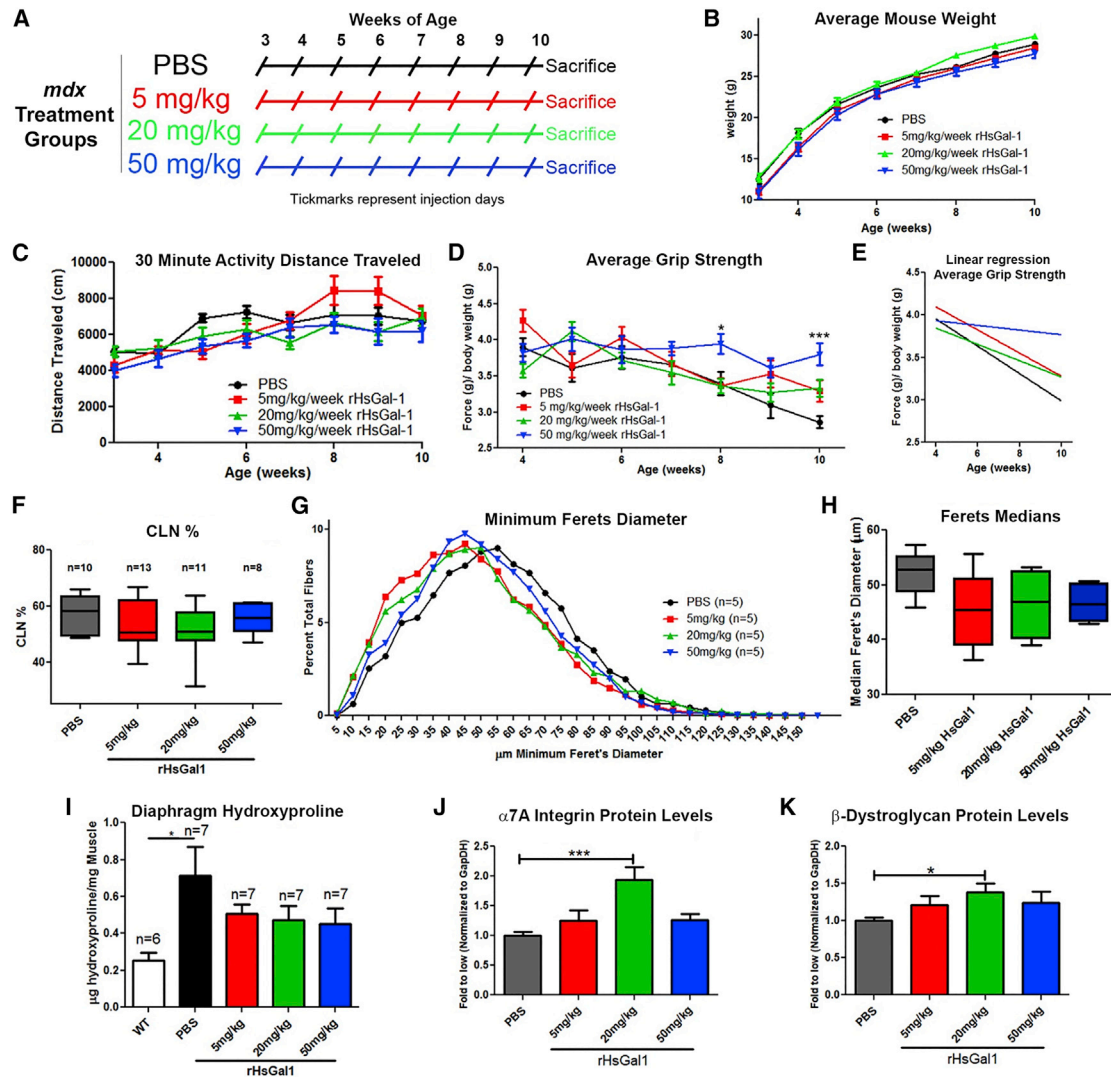**E-mail:** dburkin@medicine.nevada.edu

Figure 1. Assessment of rHsGal1 Treatments in *mdx* Mice Relative to PBS Controls

(A) The i.p. injection schedule for *mdx* mice treated with PBS and 5, 20, and 50 mg/kg rHsGal1. (B–D) Body weight (B), activity distance traveled (C), and grip strength (D) were assessed weekly in all treatment groups. (E) Linear regression assessment of the average grip strength over time. (F–H) 10-μm transverse TA muscle cryosections for all treatment groups were histologically assessed for CLN percentage (F) along with minimal Feret's fiber diameter curves (G) and median (H). (I) Diaphragm muscle from animals of all treatment groups and WT animals were biochemically assessed for collagen content using a hydroxyproline assay. (J and K) Gastrocnemius muscle extracts from animals in all treatment groups were assessed by western blotting, and the levels were quantitated for α7A Integrin (J) and β-Dystroglycan (K). Average ± SEM. Significance: *p < 0.05, **p < 0.01, ***p < 0.001.

Galectin.[11] In the present study, we examined the effects of untagged rHsGal1 on preventing disease progression in the *mdx* mouse model of DMD. rHsGal1 was purified under reducing conditions using Sepharose-lactosyl affinity and size exclusion chromatography as described previously.[30] The resulting rHsGal1 was more than 99% pure, as assessed by mass spectrometry with 0.08 endotoxin units [EUs]/mg rHsGal1 (0.8 EU/mL) endotoxin levels, meeting the Food and Drug Administration (FDA) endotoxin requirements for intravenous treatment at the concentrations used in this study. As a precaution, endo-

toxin levels were further reduced using endotoxin removal spin columns.

We determined the optimal dose of rHsGal1 treatments by i.p. delivery. i.p. treatments with PBS or 5, 20, or 50 mg/kg/week rHsGal1 into male *mdx* mice were started at 3 weeks of age and continued through to 10 weeks (Figure 1A). The body mass (Figure 1B), activity levels (Figure 1C; Figure S1), and grip strength (Figures 1D and 1E) were assessed weekly 24–48 h post-treatment, with researchers blinded to the mouse treatment groups. We observed no significant change
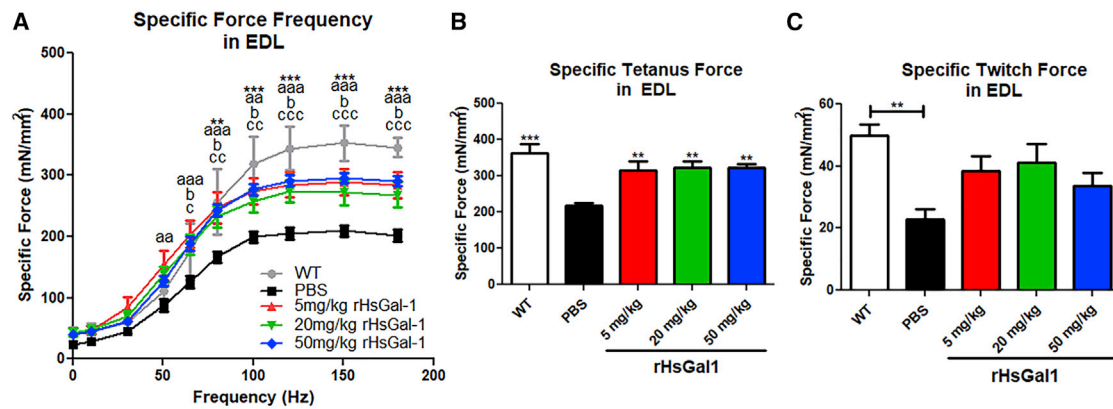
Figure 2. rHsGal1 Treatments in *mdx* Mice Improve *Ex Vivo* EDL-Specific Muscle Force Production Relative to PBS-Treated Controls

(A–C) EDL-specific force frequency (A) (significance is denoted as follows: *WT versus PBS, [a]5 mg/kg versus PBS, [b]20 mg/kg versus PBS, [c]50 mg/kg versus PBS, and [d]WT versus 20 mg/kg), specific tetanus force (B), and specific twitch force (C) production were assessed for weekly PBS (n = 8) and 5 mg/kg (n = 7), 20 mg/kg (n = 6), and 50 mg/kg (n = 6) rHsGal1 treatment groups as well as untreated WT controls (n = 6) at 10 weeks of age. Average ± SEM. Significance: *p < 0.05, **p < 0.01, ***p < 0.001.

or differences in body mass between any treatment groups during the course of this study (Figure 1B). Unlike our previous study,[11] we did not observe significant changes between any treatment groups in distance traveled in 30 min throughout the study (Figure 1C). Likewise, we observed no changes in distance traveled, resting time, or vertical breaks (Figure S1). However, at 8 and 10 weeks of age, there was a significant improvement in grip strength in *mdx* mice treated with 50 mg/kg rHsGal1 relative to the PBS treatment group (Figure 1D). Linear regression analysis for the average grip strength and/or weight over time showed significantly altered slopes (p = 0.0035), with improvements occurring in a dose-dependent manner (Figure 1E). These data show that dystrophic disease progression was slowed in rHsGal1-treated animals relative to vehicle in a dose-dependent fashion (Figure 1E).

Next, we examined the *tibialis anterior* (TA), diaphragm, and gastrocnemius muscles for histological and molecular changes with rHsGal1 treatment. The TA muscle was assessed for the percentage of myofibers with centrally located nuclei (CLNs) and myofiber size. We did not observe a significant decrease in CLNs in the TA muscle from 5, 20, or 50 mg/kg rHsGal1-treated *mdx* relative to vehicle alone (Figure 1F). However, it should be noted that we did observe a slightly lower average CLN percentage in all three rHsGal1 treatment groups, with 20 mg/kg rHsGal1-treated animals displaying the largest difference (p = 0.15) relative to PBS controls. The level of fiber hypertrophy in the TA muscle was similarly decreased with 5, 20, and 50 mg/kg rHsGal1 treatments relative to PBS, although this reduction did not reach statistical significance (Figure 1G). The median myofiber diameter fell from 52.88 μm with PBS treatment to 45.53, 46.95, or 46.58 μm in 5, 20, and 50 mg/kg rHsGal1-treated mouse groups, respectively (Figure 1H). The diaphragm muscle was used to examine changes in fibrosis using a hydroxyproline assay. As expected, we observed a significant increase in diaphragm fibrosis in PBS-treated *mdx* mice compared with untreated C57BL/10J (WT) mice (Figure 1I). The 5, 20, and 50 mg/kg rHsGal1 treatment groups exhibited

an ~30%–40% decrease in hydroxyproline content per milligram of muscle weight but were not significantly altered compared with the PBS or WT treatment groups (Figure 1I). Finally, we examined gastrocnemius muscle protein by western blotting for sarcolemma-stabilizing proteins, including α7A Integrin (Figure 1J), α7B Integrin (Figure S2), β-Dystroglycan (Figure 1K), and Utrophin (Figure S2). Both α7A Integrin (1.94-fold; Figure 1J) and β-Dystroglycan (1.39-fold; Figure 1K) protein levels were significantly elevated in the 20 mg/kg rHsGal1 treatment group relative to PBS-treated animals. Both proteins were also elevated ~20%–30% with 5 and 50 mg/kg rHsGal1 treatment relative to PBS (Figures 1J and 1K). The α7B Integrin and Utrophin protein levels were not significantly altered in any treatment group; however, the average level of both proteins was elevated in all rHsGal1 treatment groups (~20%) relative to PBS alone (Figure S2). These results show that untagged rHsGal1 IP treatments, particularly at 20 mg/kg/week, improve grip strength, decrease fiber hypertrophy, and reduce fibrosis.

Our previous study found that Galectin-1 treatment resulted in a large improvement in *ex vivo* extensor digitorum longus (EDL) muscle force production;[11] therefore, we repeated this assessment in WT and *mdx* mice treated with PBS and 5, 20, and 50 mg/kg rHsGal1. Our results showed a significant increase of ~40% in EDL-specific force frequency curves (Figure 2A) in all three *mdx* rHsGal1 treatment groups relative to the *mdx* PBS treatment group. The WT group showed the largest specific force and was significantly different from the PBS treatment group and from mice treated with rHsGal1 (Figure 2A). Similar results were observed with repeated measurements of EDL-specific tetanic force (Figure 2B), where rHsGal1 treatments restored ~67%–72% of the relative specific force lost in PBS-treated *mdx* mice compared with WT controls. The EDL-specific twitch force (Figure 2C) showed a significant difference between WT and PBS-treated *mdx* mice, but the large variability between mice failed to show significance between the control and treatment groups. However, the average specific twitch force in rHsGal1-treated *mdx* mice was
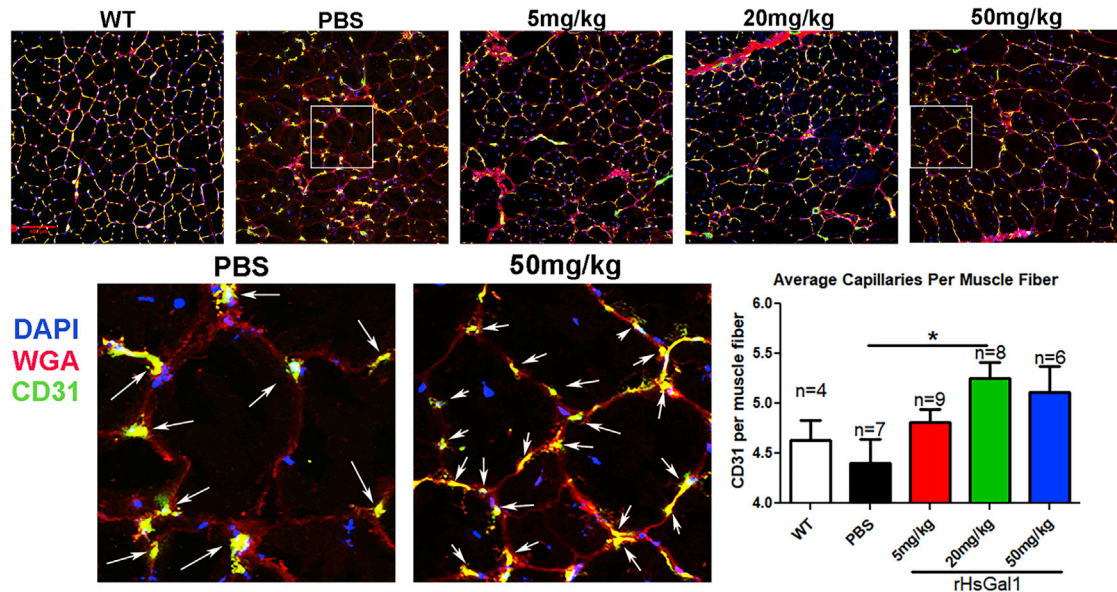
Figure 3. Weekly rHsGal1 Treatment in *mdx* Mice Increases Muscle Capillary Density

Immunofluorescent labeling of capillaries was performed using 10-μm TA cryosections from WT and all *mdx* treatment groups with Alexa Fluor 488 anti-CD31. The average number of capillaries in contact with each muscle fiber was quantitated from five 20× images for each mouse muscle section. The shaded regions from PBS and 50 mg/kg were enhanced, and capillaries are labeled with white arrows. Scale bar, 100 μm; average ± SEM. *p < 0.05.

around 40%–55% improved relative to PBS-treated controls (Figure 2C). Although we expected force to improve in a dose-dependent manner, we instead observed similar force generation across all rHsGal1 doses used in the study.

rHsGal1 Improves Capillary Density in Dystrophic Muscle

Galectin-1 has been shown previously to activate vascular growth and angiogenesis, particularly under hypoxic conditions.[25] Furthermore, improved angiogenesis in muscle has been shown to be beneficial in the *mdx* mouse model.[31] Therefore, we assessed whether systemic delivery of rHsGal1 increased vascularization of dystrophin-deficient muscle. Capillary density per muscle fiber was assessed by immunofluorescence with anti-CD31 staining in WT and *mdx* mice treated with PBS or 5, 20, and 50 mg/kg rHsGal1 (Figure 3). The capillary density observed in WT and PBS-treated *mdx* mice was similar to previously reported studies.[32] We observed a significant increase in capillary density per muscle fiber in the 20 mg/kg rHsGal1 treatment group relative to PBS-treated *mdx* animals (Figure 3). These data demonstrate that systemically delivered rHsGal1 increased muscle vascularization, which may prevent hypoxia associated with dystrophin-deficient muscle.

Assessment of the Efficacy of Intravenously Delivered rHsGal1

As a protein therapy, one of the potential paths for Galectin-1 treatment in DMD patients is through intravenous (i.v.) delivery. Therefore, we performed a small study to assess whether rHsGal1 toxicity and serum pharmacokinetics were altered from what we had observed previously with i.p. delivery.[11] No toxicity had been observed previously with rHsGal1 i.p. injections up to 50 mg/kg; therefore, we began

by assessing single-bolus retro-orbital (RO) i.v. injections of rHsGal1 at 2.5, 5, 10, 15, or 20 mg/kg (n = 3/group). Surprisingly, animals treated i.v. with concentrations of rHsGal1 above 2.5 mg/kg demonstrated acute toxicity resulting in sudden death (Figure 4A). Autopsy of these mice revealed cardiac and pulmonary blood clotting as the reason for the acute toxicity. Our analysis suggested that local blood concentrations of Galectin-1 in the bolus i.v. injection was likely above the threshold found previously to cause platelet activation and hemagglutination.[33,34] Next we examined the pharmacokinetics of 1, 2, and 3 mg/kg rHsGal1 delivered i.v. into *mdx* mice (n = 3/concentration time point) and compared this with 3 mg/kg rHsGal1 in WT mice (n = 3). We found that i.v. delivered Galectin-1 is cleared from the serum more quickly than in previous i.p. injection studies. The serum levels of rHsGal1 were depleted within ∼4 h of injection. Interestingly, the half-life serum clearance of all three injected concentrations of *mdx* (half-life [$t_{1/2}$] = 0.60–0.65) was ∼25%–30% slower than that observed in the WT ($t_{1/2}$ = 0.48). This is much faster clearance than observed previously with i.p. injections using rMsGal1, which peaked at ∼2 h with $t_{1/2}$ = 1.07 h.[11] Together, these data demonstrate that i.v. bolus injections of rHsGal1 are toxic above 2.5 mg/kg and that the muscle exposure time to the rHsGal1 is lower than with i.p. treatments.

Next we performed a small-scale efficacy study using i.v. injections with the sub-lethal dose of 2.5 mg/kg/weekly rHsGal1 in *mdx* mice, beginning at 5 weeks of age. PBS (n = 6) and rHsGal1 (n = 7) treatments began at 5 weeks, rather than earlier, because the mouse RO delivery route was too small for consistent injections prior to this age (Figure 4C). Treatments continued through 11 weeks of age,
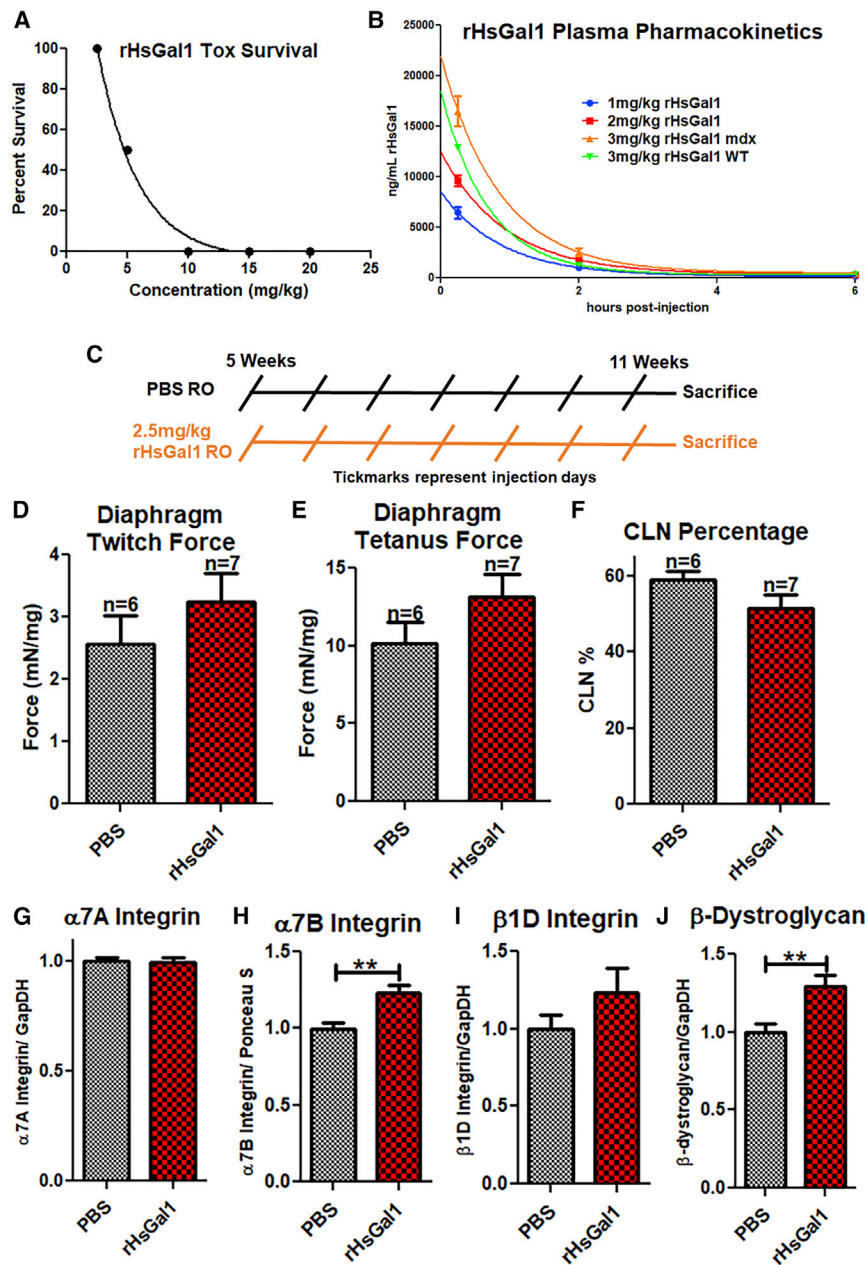
Figure 4. Assessment of i.v. rHsGal1 Treatment in *mdx* Mice

(A) i.v. rHsGal1 toxicity was assessed using 2.5, 5, 10, 15, and 20 mg/kg rHsGal1 (n = 3/treatment), followed by monitoring for 1 h. (B) The pharmacokinetics of rHsGal1 serum levels were assessed after treatments using 1, 2, and 3 mg/kg rHsGal1. Serum rHsGal1 levels were assessed by liquid chromatography-tandem mass spectrometry (LC-MS/MS) for a human-specific Galectin-1 peptide 15, 120, and 720 min post-injection. (C) A 2.5 mg/kg rHsGal1 i.v. delivery preclinical efficacy study was performed in *mdx* mice using a weekly injection schedule from 5 to 11 weeks. (D and E) Diaphragms from PBS (n = 6) and 2.5 mg/kg rHsGal1 (n = 7) treated *mdx* mice were assessed for twitch (D) and tetanus (E) force. (F) Treatment groups were assessed by immunofluorescence (IF) for CLN percentage. (G–J) Gastrocnemius sarcolemma stability protein levels were assessed by western blotting for α7A Integrin (G), α7B Integrin (H), β1D Integrin (I), and β-Dystroglycan (J). Average ± SEM.

(Figure 4G), α7B Integrin (Figure 4H), β1D Integrin (Figure 4I), and β-Dystroglycan (Figure 4J). Unlike the IP injections, we did not observe a change in α7A Integrin between the 2 treatment groups (Figure 4G). However, we did observe increased levels of α7B Integrin, β1D Integrin, and β-Dystroglycan (Figures 4H–4J), with significance between the groups in α7B Integrin and β-Dystroglycan. These data suggest that 2.5 mg/kg rHsGal1 RO injections are beneficial relative to PBS controls.

Whole-Body Pharmacodynamics of i.p. versus i.v. rHsGal1

Because we observed differences between i.p. versus i.v. pharmacokinetics, we decided to examine the pharmacodynamics of fluorescently labeled rHsGal1 in CD1 mice. A pretreatment image was taken from all mice, and, as expected, none possessed any signal at the imaging setting used for data collection (Figure 5A). The mice were then injected with 2.5 mg/kg Dylight-650-labeled rHsGal1 (650-rHsGal1) by either i.p. or i.v. injection. The CD1 mice were then imaged immediately using the *in vivo* imaging system (IVIS), which demonstrated a slow distribution of 650-rHsGal1 into systemic tissues from the injection site in the i.p. injected mouse (Figure 5B). Conversely, the 650-rHsGal1 injected i.v. was immediately observed to be present throughout the entire mouse (Figure 5E). Finally, we again examined all 650-rHsGal1-injected mice by IVIS 4 h later, with both ventral and dorsal views (Figures 5C, 5D, 5F, and 5G). Interestingly, the 650-rHsGal1 i.p. injection had spread throughout the body with noticeably brighter spots in the bladder and kidneys (Figures 5C and 5D). The 650-rHsGal1 i.v.

when *ex vivo* contraction studies (Figures 4D and 4E) were performed on diaphragm muscle. The diaphragm was chosen for examination because it is generally considered to be the most affected muscle in *mdx* mice at 10–11 weeks of age. We found a slight improvement with rHsGal1 treatments relative to PBS in both twitch (Figure 4D) and tetanus-specific force (Figure 4E); however, neither was significantly improved. We then examined the CLN percentage in the TA between the two treatment groups. We found a non-significant 7% decrease in CLN percentage in the rHsGal1 treatment group relative to PBS-treated *mdx* mice (Figure 4F). The gastrocnemius muscles were then assessed by western blotting for the levels of α7A Integrin
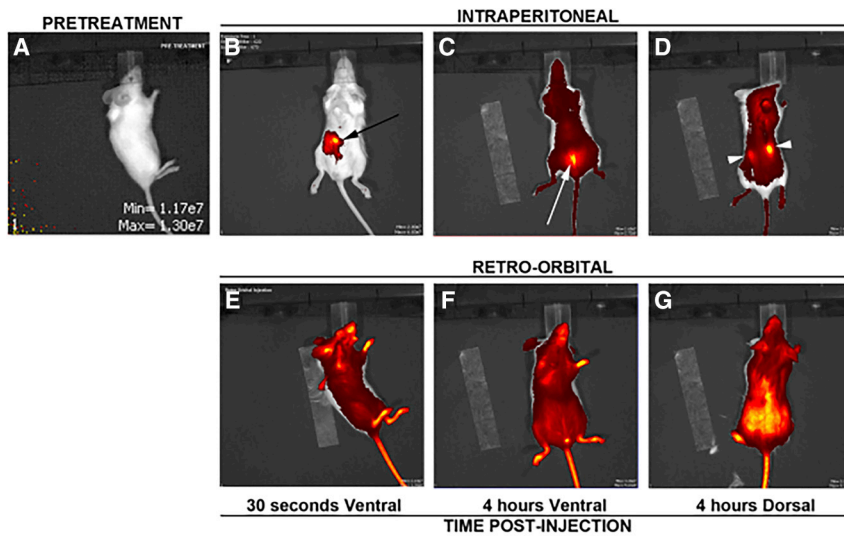
Figure 5. Dynamics of Alexa Fluor 488-Labeled rHsGal1 i.p. and i.v. Injections 1 min and 4 h Post-injection

(A) IVIS representative pretreatment image. (B–G) After 2.5 mg/kg Alexa Fluor 488-labeled rHsGal1 treatment either i.p. (B–D) or i.v. (E–G) a ventral (B, C, E, and F) or dorsal (D and G) image was taken using IVIS either 30 s (B and E) or 4 h (C, D, F, and G) post-injection. The black arrow corresponds to the i.p. injection site, the white arrow indicates the bladder, and the white arrowheads depict the kidneys.

injection retained large amounts of signal throughout the animal, with elevated levels appearing in the dorsal view (Figures 5F and 5G). The cage with 650-rHsGal1 i.v. injected animals had notably blue bedding at 4 h, indicating that a significant amount of labeled rHsGal1 had already passed through the bladder and been excreted.

DISCUSSION

Galectin-1 is a novel biological agent that has efficacy in slowing disease progression in preclinical murine models of DMD. In this study, we investigated the optimal dosing and delivery of rHsGal1 in the *mdx* mouse model of DMD. Optimal i.p. dosing was determined to be 20 mg/kg/week rHsGal1 using physiological, molecular, and histological outcome measures. However, it should be noted that we did not attempt more frequent dosing schedules, which may be warranted based on rHsGal1 serum clearance. Grip strength assessment showed a correlation between escalating doses and strength improvement over time. Other measurements, including CLN, muscle fiber size, diaphragm fibrosis, and *ex vivo* EDL muscle force assessments, suggested equal improvements across all rHsGal1 treatment groups. Finally, western blots and capillary density data suggested that maximum benefits were achieved using 20 mg/kg/week rHsGal1, the same dose found previously to be optimal with mouse Galectin-1 treatments.[11] Together, these studies provide a foundation for further dose evaluation studies and confirm the therapeutic value of Galectin-1 treatments for DMD.

In the current study, the actimetry, histologically assessed CLN, and Utrophin protein levels failed to achieve the significance observed previously.[11] There are several potential reasons why these discrepancies between treatments may have occurred. The first and most likely is due to differences between the Galectin-1 production methods and the recombinant proteins themselves. This study used DTT to maintain Galectin-1 in a reduced form, which has been suggested to be more active than oxidized versions.[26,33,35] It has been shown previously that the oxidized and reduced forms of Galectin-1 can have highly different *in vivo* activities,[36,37] and it is possible that the oxidized version was used previously with altered effects. It is also possible that the amino acid sequence differences between mouse and human Galectin-1 cause protein interaction differences in the mouse host. The results from this study clearly show that human Galectin-1 treatment did induce an immune response against the injected protein. Therefore, it is also possible that rHsGal1 protein does not provide the same long-term sarcolemma stability found previously because of expedited clearance.

Functional ischemic muscle conditions in DMD patients and dystrophin-deficient animal models have long been thought to contribute to disease progression.[38] Our data suggest that rHsGal1 treatments may alter the capillary density-to-muscle fiber ratio. This fits with previous reports that Galectin-1 can directly interact with VEGFR2 and positively increase angiogenesis.[39] Because *mdx* and golden retriever models of DMD have reduced capillary density and muscle ischemia,[40,41] our results suggest that this could be a direct mechanism by which Galectin-1 treatment improves *mdx* outcome measures. Galectin-1 could be particularly effective when used in conjunction with phosphodiesterase-5 inhibitors,[42] which will improve blood flow through nitric oxide (NO)-induced vessel relaxation.

The i.v. studies identified a limit to the maximum dose of rHsGal1 that should be used by this method of delivery and indicates careful dosing to avoid a high local concentration of rHsGal1 in the blood. This toxicity was not observed with i.p. delivery (even at 100 mg/kg), which resulted in a slower increase in Galectin-1 in the blood and, thus, from the blood to the skeletal muscle. i.p. delivery also resulted in a longer half-life, which was likely due to this slow distribution into the blood, and also led to better outcome measures. These data suggest a pharmacokinetic model in which the distribution of rHsGal1 from the blood into the skeletal muscle compartment is a slow process and is maximally activated at lower Galectin-1 concentrations. If Galectin-1 distribution into muscle is rate-limited, then a delivery method that results in sustained blood levels of blood Galectin-1 would result in the largest accumulation in muscle tissue.

This is what was observed in our subcutaneous or i.p. dosing, which, therefore, would be more efficacious for treating DMD patients and would also mitigate the toxicity risk observed by large-bolus i.v. injections. Additionally, developing Galectin-1 as a subcutaneously delivered therapeutic agent would be beneficial for patients because regular treatments could be performed at home using autoinjectors instead of requiring regular i.v. infusions in a clinic.

We believe that the toxicity resulting from cardio-pulmonary clotting and asphyxiation occurred because of Galectin-1 triggering platelet activation, which is dependent on the lectin-binding activities of rHsGal1.[34] Interestingly, this may not be an issue with the oxidized version of Galectin-1, which has been reported to lack the lectin-binding potential of the reduced form.[33] Therefore, slower delivery and control of rHsGal1 in the bloodstream by subcutaneous delivery may prevent this adverse reaction to i.v. delivery as we continue to develop an rHsGal1 therapeutic agent for DMD. Additionally, optimizing the pharmacokinetics of Galectin-1 by addition of a polyethylene glycol (PEG) or other moiety could also increase the efficacy of Galectin-1. This study has expanded our understanding of the mechanistic action of Galectin-1 as a therapeutic treatment for DMD and suggests future experiments for optimization of both efficacy and safety.

MATERIALS AND METHODS

Human Galectin-1 Expression, Purification, and Evaluation

The human galectin-1 (LGALS1) cDNA was produced using reverse transcriptase (Superscript III, Invitrogen) from HeLa cell total RNA (Trizol, Invitrogen) followed by PCR using Platinum Taq Supermix (Invitrogen). The human LGALS1 cDNA was initially cloned into the pET23b (EMD Millipore) vector (the normal stop codon preventing C-terminal His_6 tag translation), transformed into Rosetta *E. coli* (EMD Millipore), grown for ∼22 h in 2× yeast extract tryptone (2×YT) medium, and induced for rHsGal1 expression using 0.4 mM isopropyl-β-D-1-thiogalactopyranoside (IPTG) (Invitrogen). Five hours post-induction, the bacteria were pelleted by light centrifugation, resuspended in PBS + protease inhibitor cocktail set III (Calbiochem) + 8 mM DTT (Genesee), and lysed through sonication. The lysate was cleared of nonessential cell debris by ultracentrifugation and then affinity-purified over a β-lactosyl Sepharose 6B column using ACTApure fast protein liquid chromatography (FPLC) (GE Healthcare) as described previously.[30] Fractions containing rHsGal1 were then run over a Sephacryl S-100 column or twice through Proteus NoEndoS removal columns (Charles River Laboratories). The purified rHsGal1 was assessed by mass spectrometry for identity and purity, the Pierce LAL Chromogenic Endotoxin Quantitation Kit for endotoxin levels, western blotting to follow the protein during FPLC fractionation (see below), and Coomassie staining for purity.

Animals

mdx (C57Bl/10ScSn-Dmd^mdx) and WT (C57BL/10ScSn) mouse housing and experiments were performed under an approved protocol from the University of Nevada, Reno Institutional Animal Care and Use Committee (IACUC) under guidelines set forth by the NIH. In the dose escalation study, 3-week-old male *mdx* mice were treated weekly with a single injection of PBS or 5, 20, or 50 mg/kg rHsGal1. Body weight was monitored every week. Forelimb grip strength and activity data were collected weekly from 4 weeks of age to 10 weeks of age as described previously.[11] At the end of the study, the EDL muscle was appropriately harvested for *ex vivo* contraction studies prior to final sacrifice and harvesting of other muscle tissues. All RO injections and serum blood draws were performed under isoflurane anesthesia. The RO toxicity study was initiated with 2.5, 5, 10, 15, and 20 mg/kg rHsGal1 after unexpected complications with the initial 20 mg/kg rHsGal1 i.v. injections. All animals were treated according to the rules and regulations specified by the IACUC. At the end of the study, the diaphragm of the mice were appropriately harvested for either contractile measurements or phrenic nerve stimulation and recording studies.

Mouse Activity Assessments

Activity assessments were performed as described previously.[11] Experiments were performed weekly, 24 h post-treatment, by placing mice in the Opto-Varimex-4 system with Auto-track v4.96 software for a 30-min time period (Columbus Instruments).

Mouse Forelimb Grip Strength

Grip strength was assessed as described previously.[11] Mouse grip strength was determined using a San Diego Instruments (SDI) grip strength system and a Chatillon digital force gauge tensometer. Grip strength testing was performed six times, with 30-s rest periods between pulls, by a member of the Burkin lab blinded to treatment groups.

Ex Vivo EDL and Diaphragm Muscle Strength Assessment

EDL and diaphragm muscle strength analysis was assessed as described previously.[11,43] Briefly, muscles were mounted in an oxygenated tissue bath in a physiological salt solution and hung from a computer-controlled Aurora Scientific servomotor. After acclimation, 3 isometric twitch (1 Hz) and 3 isometric tetanus (150 Hz) contractions and force frequency (10, 30, 50, 65, 80, 100, 120, 150, and 180 Hz) protocols were performed. There was a 10-min rest between each set of experiments. All experiments used an electrical stimulation of 7 V with a 200-μs pulse duration (701A Stimulator, Aurora Scientific).

Cryosectioning

A Leica CM1850 cryostat was used with Tissue-TEK optimal cutting temperature compound-embedded TA muscles (Sakura Finetek USA) as described previously.[11]

Histological Assessment

10-μm TA sections were blocked in 5% BSA (Fisher Scientific), stained with Alexa Fluor 488 wheat germ agglutinin (WGA) (Molecular Probes, Invitrogen Detection Technologies), and mounted in Vectashield Hard Set with DAPI (Vector Laboratories, Burlingame, CA). Images were captured using a Zeiss Axioskop 2 Plus fluorescence microscope, a Zeiss AxioCam HRc digital camera, and Axiovision

4.8 software or an Olympus FluoviewFV1000 laser-scanning biological confocal microscope using the Olympus Micro FV10-ASW 3.1 software. CLN percentage and Feret's minimal diameter were measured after stitching together images to recreate a montage of the entire TA muscle section.

Immunofluorescence

Immunostaining was performed as described previously.[11] Briefly, 10-μm TA sections were blocked with 5% BSA and then incubated using antibodies against total α7 integrin, β1D Integrin, β-Dystroglycan, and Utrophin as described previously, followed by fluorescein isothiocyanate (FITC) donkey anti-rabbit (1:1,000, Jackson ImmunoResearch, Baltimore, MD) and mounting using Vectashield containing DAPI (H-1500, Vector Laboratories, CA). Images were taken as described previously. Capillary staining was performed using Alexa Fluor 488 anti-mouse CD31 (BioLegend, 102513).

Immunoblotting

Crushed gastrocnemius muscles were suspended in radioimmunoprecipitation assay (RIPA) buffer plus protease inhibitor cocktail set III (Calbiochem) and allowed to dissociate on ice for 30 min. Insoluble material was removed by centrifugation, and protein concentration was determined by bicinchoninic acid (BCA).[11] Varying amounts of protein extract (5 μg for α7A and α7B Integrin, 10 mg for β-Dystroglycan, and 30 mg for β1D Integrin and Utrophin) were loaded per lane, separated on SDS-PAGE gels, and transferred to nitrocellulose. All blots were blocked in 2% BSA, which was also used to dilute antibodies. Blots were probed using α7A and α7B integrin-specific rabbit polyclonal antibody, β-Dystroglycan H-242 (sc-28535, 1:200), β1D Integrin, utrophin (MANCHO3, 1:50, Developmental Studies Hydridoma Bank [DSHB]), and Galectin-1 (1:100, New England Peptide) and normalized to either glyceraldehyde 3-phosphate dehydrogenase (GAPDH V-18, sc-20357, 1:200) or α-tubulin (DM1A, ab7291, Abnova,1:500). Primary antibodies were detected using Alexa Fluor 680 goat anti-rabbit immunoglobulin G (IgG), Alexa Fluor 800 donkey anti-rabbit IgG, Alexa Fluor 800 goat anti-mouse IgG, and Alexa Fluor 800 or 680 donkey anti-goat IgG (1:5,000 Molecular Probes, Invitrogen Detection Technologies).

Hydroxyproline Assay

The assay was performed as described previously.[11] Briefly, cleaned diaphragm samples were weighed and incubated overnight (O/N) at 110°C in 2 mL of 6 N HCl. 10 μL of the resulting hydrolysate sample was then mixed with 150 μL isopropanol and then 72 μL chloramine T reagent and incubated for 10 min at room temperature (RT) to allow oxidation. 1,000 μL of freshly prepared Ehrlich's reagent was then added, and samples were incubated at 55°C for 30 min. 200 μL of each sample was transferred to a clear 96-well plate. Samples were run in triplicate, and absorbance was measured at 550 nm.

Labeled rHsGal1 Mouse Dynamics

The Dylight-650 NHS Labeling Kit (Thermo Fisher Scientific, 46403) was used to label rHsGal1. CD1 mice were injected either RO or i.p.

and immediately scanned for the Dylight-650 signal using an IVIS (PerkinElmer). Four hours later, the mice were scanned again.

Statistical Analysis and Curve Fitting

Statistical analysis was performed with GraphPad Prism software using one-way or two-way ANOVA followed by a Bonferroni comparison between all treatment groups. GraphPad prism software was also used to fit curves using nonlinear regression analysis and to provide half-life measurements in the pharmacokinetics (PK) study. Error bars in all figures represent SEM. Significance is displayed as follows: $^*p < 0.05$, $^{**}p < 0.01$, $^{***}p < 0.001$.

SUPPLEMENTAL INFORMATION

Supplemental Information includes five figures and can be found with this article online at https://doi.org/10.1016/j.omtm.2019.01.004.

AUTHOR CONTRIBUTIONS

Conceptualization, R.D.W. and D.J.B.; Methodology, R.D.W., P.V.R., P.D.B., and P.J.; Investigation, R.D.W., V.C., P.V.R., P.B.-F., P.D.B., and P.J.; Writing – Original Draft, R.D.W.; Writing – Review & Editing, R.D.W., D.J.B., P.V.R., and P.D.B.; Funding Acquisition, D.J.B. and R.D.W.; Supervision, R.D.W. and D.J.B.

CONFLICTS OF INTEREST

The University of Nevada, Reno has been issued a patent for the therapeutic use of Galectin-1 for the treatment of muscle disease. The University of Nevada, Reno has licensed this technology to StrykaGen Corp., Reno, NV, which is owned by D.J.B. and R.D.W. The University of Nevada, Reno has a small equity share in this company.

ACKNOWLEDGMENTS

REFERENCES

1. Bello, L., Morgenroth, L.P., Gordish-Dressman, H., Hoffman, E.P., McDonald, C.M., and Cirak, S.; CINRG investigators (2016). DMD genotypes and loss of ambulation in the CINRG Duchenne Natural History Study. Neurology 87, 401–409.

2. Guiraud, S., Aartsma-Rus, A., Vieira, N.M., Davies, K.E., van Ommen, G.J., and Kunkel, L.M. (2015). The Pathogenesis and Therapy of Muscular Dystrophies. Annu. Rev. Genomics Hum. Genet. 16, 281–308.

3. Angelini, C., Pegoraro, E., Turella, E., Intino, M.T., Pini, A., and Costa, C. (1994). Deflazacort in Duchenne dystrophy: study of long-term effect. Muscle Nerve 17, 386–391.

4. Beenakker, E.A., Fock, J.M., Van Tol, M.J., Maurits, N.M., Koopman, H.M., Brouwer, O.F., and Van der Hoeven, J.H. (2005). Intermittent prednisone therapy in Duchenne muscular dystrophy: a randomized controlled trial. Arch. Neurol. 62, 128–132.

5. Fenichel, G.M., Florence, J.M., Pestronk, A., Mendell, J.R., Moxley, R.T., 3rd, Griggs, R.C., Brooke, M.H., Miller, J.P., Robison, J., King, W., et al. (1991). Long-term benefit from prednisone therapy in Duchenne muscular dystrophy. Neurology 41, 1874–1877.

6. Fenichel, G.M., Mendell, J.R., Moxley, R.T., 3rd, Griggs, R.C., Brooke, M.H., Miller, J.P., Pestronk, A., Robison, J., King, W., Signore, L., et al. (1991). A comparison of daily and alternate-day prednisone therapy in the treatment of Duchenne muscular dystrophy. Arch. Neurol. 48, 575–579.

7. Reitter, B. (1995). Deflazacort vs. prednisone in Duchenne muscular dystrophy: trends of an ongoing study. Brain Dev. 17 (Suppl), 39–43.

8. Wuebbles, R.D., Sarathy, A., Kornegay, J.N., and Burkin, D.J. (2013). Levels of α7 integrin and laminin-α2 are increased following prednisone treatment in the mdx mouse and GRMD dog models of Duchenne muscular dystrophy. Dis. Model. Mech. 6, 1175–1184.

9. Malik, V., Rodino-Klapac, L.R., and Mendell, J.R. (2012). Emerging drugs for Duchenne muscular dystrophy. Expert Opin. Emerg. Drugs 17, 261–277.

10. Spinazzola, J.M., and Kunkel, L.M. (2016). Pharmacological therapeutics targeting the secondary defects and downstream pathology of Duchenne muscular dystrophy. Expert Opin. Orphan Drugs 4, 1179–1194.

11. Van Ry, P.M., Wuebbles, R.D., Key, M., and Burkin, D.J. (2015). Galectin-1 Protein Therapy Prevents Pathology and Improves Muscle Function in the mdx Mouse Model of Duchenne Muscular Dystrophy. Mol. Ther. 23, 1285–1297.

12. Camby, I., Le Mercier, M., Lefranc, F., and Kiss, R. (2006). Galectin-1: a small protein with major functions. Glycobiology 16, 137R–157R.

13. Matsumura, C.Y., Menezes de Oliveira, B., Durbeej, M., and Marques, M.J. (2013). Isobaric Tagging-Based Quantification for Proteomic Analysis: A Comparative Study of Spared and Affected Muscles from mdx Mice at the Early Phase of Dystrophy. PLoS ONE 8, e65831.

14. Barrientos, G., Freitag, N., Tirado-González, I., Unverdorben, L., Jeschke, U., Thijssen, V.L., and Blois, S.M. (2014). Involvement of galectin-1 in reproduction: past, present and future. Hum. Reprod. Update 20, 175–193.

15. Hu, Z., Liang, M.C., and Soong, T.W. (2017). Alternative Splicing of L-type Ca$_V$1.2 Calcium Channels: Implications in Cardiovascular Diseases. Genes (Basel) 8, E344.

16. Wang, J., Thio, S.S., Yang, S.S., Yu, D., Yu, C.Y., Wong, Y.P., Liao, P., Li, S., and Soong, T.W. (2011). Splice variant specific modulation of CaV1.2 calcium channel by galectin-1 regulates arterial constriction. Circ. Res. 109, 1250–1258.

17. Cha, S.K., Ortega, B., Kurosu, H., Rosenblatt, K.P., Kuro-O, M., and Huang, C.L. (2008). Removal of sialic acid involving Klotho causes cell-surface retention of TRPV5 channel via binding to galectin-1. Proc. Natl. Acad. Sci. USA 105, 9805–9810.

18. Chan, J., O'Donoghue, K., Gavina, M., Torrente, Y., Kennea, N., Mehmet, H., Stewart, H., Watt, D.J., Morgan, J.E., and Fisk, N.M. (2006). Galectin-1 induces skeletal muscle differentiation in human fetal mesenchymal stem cells and increases muscle regeneration. Stem Cells 24, 1879–1891.

19. Georgiadis, V., Stewart, H.J., Pollard, H.J., Tavsanoglu, Y., Prasad, R., Horwood, J., Deltour, L., Goldring, K., Poirier, F., and Lawrence-Watt, D.J. (2007). Lack of galectin-1 results in defects in myoblast fusion and muscle regeneration. Dev. Dyn. 236, 1014–1024.

20. Gu, M., Wang, W., Song, W.K., Cooper, D.N., and Kaufman, S.J. (1994). Selective modulation of the interaction of alpha 7 beta 1 integrin with fibronectin and laminin by L-14 lectin during skeletal muscle differentiation. J. Cell Sci. 107, 175–181.

21. Kami, K., and Senba, E. (2005). Galectin-1 is a novel factor that regulates myotube growth in regenerating skeletal muscles. Curr. Drug Targets 6, 395–405.

22. Watt, D.J., Jones, G.E., and Goldring, K. (2002). The involvement of galectin-1 in skeletal muscle determination, differentiation and regeneration. Glycoconj. J. 19, 615–619.

23. Moiseeva, E.P., Williams, B., Goodall, A.H., and Samani, N.J. (2003). Galectin-1 interacts with beta-1 subunit of integrin. Biochem. Biophys. Res. Commun. 310, 1010–1016.

24. Thijssen, V.L., and Griffioen, A.W. (2014). Galectin-1 and -9 in angiogenesis: a sweet couple. Glycobiology 24, 915–920.

25. van Beijnum, J.R., Thijssen, V.L., Läppchen, T., Wong, T.J., Verel, I., Engbersen, M., Schulkens, I.A., Rossin, R., Grüll, H., Griffioen, A.W., and Nowak-Sliwinska, P. (2016). A key role for galectin-1 in sprouting angiogenesis revealed by novel rationally designed antibodies. Int. J. Cancer 139, 824–835.

26. Chang-Hong, R., Wada, M., Koyama, S., Kimura, H., Arawaka, S., Kawanami, T., Kurita, K., Kadoya, T., Aoki, M., Itoyama, Y., and Kato, T. (2005). Neuroprotective effect of oxidized galectin-1 in a transgenic mouse model of amyotrophic lateral sclerosis. Exp. Neurol. 194, 203–211.

27. Horie, H., Inagaki, Y., Sohma, Y., Nozawa, R., Okawa, K., Hasegawa, M., Muramatsu, N., Kawano, H., Horie, M., Koyama, H., et al. (1999). Galectin-1 regulates initial axonal growth in peripheral nerves after axotomy. J. Neurosci. 19, 9964–9974.

28. Toscano, M.A., Campagna, L., Molinero, L.L., Cerliani, J.P., Croci, D.O., Ilarregui, J.M., Fuertes, M.B., Nojek, I.M., Fededa, J.P., Zwirner, N.W., et al. (2011). Nuclear factor (NF)-κB controls expression of the immunoregulatory glycan-binding protein galectin-1. Mol. Immunol. 48, 1940–1949.

29. Ito, K., Stannard, K., Gabutero, E., Clark, A.M., Neo, S.Y., Onturk, S., Blanchard, H., and Ralph, S.J. (2012). Galectin-1 as a potent target for cancer therapy: role in the tumor microenvironment. Cancer Metastasis Rev. 31, 763–778.

30. Fouillit, M., Lévi-Strauss, M., Giudicelli, V., Lutomski, D., Bladier, D., Caron, M., and Joubert-Caron, R. (1998). Affinity purification and characterization of recombinant human galectin-1. J. Chromatogr. B Biomed. Sci. Appl. 706, 167–171.

31. Messina, S., Mazzeo, A., Bitto, A., Aguennouz, M., Migliorato, A., De Pasquale, M.G., Minutoli, L., Altavilla, D., Zentilin, L., Giacca, M., et al. (2007). VEGF overexpression via adeno-associated virus gene transfer promotes skeletal muscle regeneration and enhances muscle function in mdx mice. FASEB J. 21, 3737–3746.

32. Burch, T.G., Prewitt, R.L., and Law, P.K. (1981). In vivo morphometric analysis of muscle microcirculation in dystrophic mice. Muscle Nerve 4, 420–424.

33. Inagaki, Y., Sohma, Y., Horie, H., Nozawa, R., and Kadoya, T. (2000). Oxidized galectin-1 promotes axonal regeneration in peripheral nerves but does not possess lectin properties. Eur. J. Biochem. 267, 2955–2964.

34. Pacienza, N., Pozner, R.G., Bianco, G.A., D'Atri, L.P., Croci, D.O., Negrotto, S., Malaver, E., Gómez, R.M., Rabinovich, G.A., and Schattner, M. (2008). The immunoregulatory glycan-binding protein galectin-1 triggers human platelet activation. FASEB J. 22, 1113–1123.

35. Guardia, C.M., Caramelo, J.J., Trujillo, M., Méndez-Huergo, S.P., Radi, R., Estrin, D.A., and Rabinovich, G.A. (2014). Structural basis of redox-dependent modulation of galectin-1 dynamics and function. Glycobiology 24, 428–441.

36. Cedeno-Laurent, F., and Dimitroff, C.J. (2012). Galectin-1 research in T cell immunity: past, present and future. Clin. Immunol. 142, 107–116.

37. Yu, X., Scott, S.A., Pritchard, R., Houston, T.A., Ralph, S.J., and Blanchard, H. (2015). Redox state influence on human galectin-1 function. Biochimie 116, 8–16.

38. Sander, M., Chavoshan, B., Harris, S.A., Iannaccone, S.T., Stull, J.T., Thomas, G.D., and Victor, R.G. (2000). Functional muscle ischemia in neuronal nitric oxide synthase-deficient skeletal muscle of children with Duchenne muscular dystrophy. Proc. Natl. Acad. Sci. USA 97, 13818–13823.

39. Stanley, P. (2014). Galectin-1 Pulls the Strings on VEGFR2. Cell 156, 625–626.

40. Nguyen, F., Guigand, L., Goubault-Leroux, I., Wyers, M., and Cherel, Y. (2005). Microvessel density in muscles of dogs with golden retriever muscular dystrophy. Neuromuscul. Disord. 15, 154–163.

41. Palladino, M., Gatto, I., Neri, V., Straino, S., Smith, R.C., Silver, M., Gaetani, E., Marcantoni, M., Giarretta, I., Stigliano, E., et al. (2013). Angiogenic impairment of the vascular endothelium: a novel mechanism and potential therapeutic target in muscular dystrophy. Arterioscler. Thromb. Vasc. Biol. 33, 2867–2876.

42. Asai, A., Sahani, N., Kaneki, M., Ouchi, Y., Martyn, J.A., and Yasuhara, S.E. (2007). Primary role of functional ischemia, quantitative evidence for the two-hit mechanism, and phosphodiesterase-5 inhibitor therapy in mouse muscular dystrophy. PLoS ONE 2, e806.

43. Sarathy, A., Wuebbles, R.D., Fontelonga, T.M., Tarchione, A.R., Mathews Griner, L.A., Heredia, D.J., Nunes, A.M., Duan, S., Brewer, P.D., Van Ry, T., et al. (2017). SU9516 Increases α7β1 Integrin and Ameliorates Disease Progression in the mdx Mouse Model of Duchenne Muscular Dystrophy. Mol. Ther. 25, 1395–1407.